

## Final Science Report

### University of Minnesota High Altitude X-ray Detector Testbed Payload High Altitude Student Platform – 2018

#### Points of Contact:

Kyle J. Houser <house253@umn.edu>

Abigail Valero <valer044@umn.edu>

Jenna Burgett <burge241@umn.edu>

#### Faculty Advisors:

Demoz Gebre-Egziabher

Lindsay Glesener

Gerald Sobelman

University of Minnesota – Twin Cities

### Abstract

This document discusses the results and conclusions obtained from the 2018 High Altitude Student Platform (HASP) flight of the University of Minnesota's High Altitude X-ray Detector Testbed (HAXDT). The 2018 HAXDT main payload hosted the CsI(Tl) Incident Energy Spectrometer (CITIES) developed by the University of Minnesota Small Satellite Research Lab. This X-ray and gamma-ray detector is being developed as an effort to create a dual-use CubeSat sensor for the characterization of high energy photons from astrophysical sources and for making position, navigation and timing (PNT) measurements. This year's flight was meant to validate the functionality of a Field Programmable Gate Array (FPGA) in the CITIES detector system as well as test the reprogramming of the flight computer via onboard radios during flight. The current design of the main payload closely resembles the final iteration of CITIES and its supporting hardware that will be implemented into two University-built CubeSats<sup>1</sup>. This year's flight proved to be crucial for the characterization of performance for the system as a whole. An engineering analysis of the main payload's subsystems was also performed. These subsystems included the communications, flight computer, and electrical and power systems. HAXDT is designed in the form-factor of a 3U CubeSat so that the whole system mimics the designs of the two CubeSats currently being developed by the small satellite research group as much as possible. Consequently, this engineering test provided valuable insight into the performance of the integrated subsystems which will then be utilized to optimize the payload design for future iterations. This year's HAXDT also included a secondary payload including an AlphaSense optical particle counter (OPC). More information about the secondary payload is found in Appendix A.

---

<sup>1</sup> The University of Minnesota is currently building two 3U CubeSats: EXACT (Experiment for X-ray Characterization and Timing) and SOCRATES (Signal of Opportunity CubeSat Ranging and Timing Experiments). Components for these CubeSats are being tested on HAXDT.

## Introduction

The main purpose of the University of Minnesota's High Altitude X-Ray Testbed (HAXDT) for the 2018 flight of the High Altitude Student Platform (HASP) was to test the performance of the CsI(Tl) Incident Energy Spectrometer (CITIES) and its supporting hardware in a space-like environment. This detector has been designed and optimized to detect X-ray and gamma-ray emissions from astrophysical sources including the sun, pulsars, and X-ray binary systems in the hopes of studying solar flares and developing a Guidance, Navigation and Control (GNC) sensor. The development of CITIES has focused for the past 8 years on conceiving an X-ray and gamma-ray detector for implementation in nanosatellites. Previous iterations of the sensor have been tested in HASP [1, 2] and the lessons learned from those tests have been used to optimize the most recent prototype. The sensor itself aims to fulfill two separate goals with similar requirements: a scientific goal and an engineering goal.

As a science instrument, CITIES studies the solar flare events from the sun and characterizes the high energy photons emitted by said events. When looking at the sun, CITIES focuses on X-ray photon energies and arrival times that will enable the study of electron acceleration in solar flares. This will allow for further understanding of space weather and could provide key information as to why the corona of the sun has a significantly higher temperature than the surface of the sun. The understanding and modeling these events is of great importance as they pose a threat to satellites, astronauts, and power grids on Earth. Exposure to the electromagnetic radiation and energetic particles released by these flares, experienced by astronauts orbiting in the International Space Station (ISS), could result in an increased chance of major health issues, including cancer. These particles can also collide with crucial electronics in satellites and damage vital components of the system. Similarly, the flares can also cause electromagnetic fluctuations in the Earth's atmosphere that can induce electric fluctuations in the power grids and blow out transformers.

As an engineering sensor, CITIES will measure gamma-ray photons emitted by Gamma Ray Bursts (GRBs) in an attempt to make position, navigation, and timing (PNT) measurements [3]. GRBs emit radiation concentrated in the gamma-ray band of the electromagnetic spectrum at a rate of around once per day. The arrival times of these emissions in multiple spatially separated detectors can be used to determine a relative position solution using the time difference of arrival (TDOA). The goal is to eventually use CITIES in a 3U CubeSat to measure these gamma-ray emissions and compute a relative position solution for the satellite based on the on-board measurements and measurements found by other spacecraft which are currently in orbit. This technology would prove to be useful in deep-space missions where the spacecraft is outside the sphere of influence of GNSS satellites. This technology has already been identified by NASA as a NASA technology requirement [4].

The main HAXDT payload serves as a testbed for CITIES, and it is currently designed in the form factor of a 3U CubeSat in an effort to closely resemble the integrated subsystems that will be used

in the EXACT and SOCRATES missions. Consequently, the HASP flight also serves as an engineering test for these integrated subsystems and provides valuable information regarding the design of the satellites. As a result of the 2018 flight, the University of Minnesota (UMN) team has been able to validate many subsystem designs and will finalize iterations of these systems ahead of the SOCRATES satellite launch planned for 2019 from the ISS. Data from this flight was used to validate the use of the FPGA as a means of data processing and curve fitting of incoming signals generated by the detector. With the addition of the FPGA, the flight computer no longer has to handle raw data coming from the detector, leading to increased data sample rates and data compression. The reprogramming of the flight computer via radio was also achieved by this iteration of HAXDT. This will provide a way to fix and change flight computer code during flight.

### CITIES Description

The experiment described in this report was designed to conform to the power and interference requirements of Louisiana State University's (LSU) HASP while still maintaining the form factor of a 3U CubeSat as much as possible. The driving requirements of the detector subsystem were determined by the science goals of EXACT and SOCRATES so that each mission can be successful. There are four major driving requirements for CITIES:

- 1) CITIES shall measure the energy of incident X-ray photons with at least 25% resolution in the energy regime of 10-100 keV as dictated by the primary mission science requirements.
- 2) CITIES shall have at least 25 cm<sup>2</sup> of detection area between 16 channels of detection.
- 3) CITIES shall measure the time of arrival of incident photons to at least 25ms accuracy.
- 4) CITIES shall process 8000 photons per second between 16 channels of detection.

The requirements in energy resolution and total detection area have the most influence over the design of the system. In order to gain high detection area, a scintillation detector design was chosen as a large detection area can be obtained for relatively low cost by the replication of a single channel. Scintillation detectors take advantage of large crystals, CsI for this design, which are activated with a dopant, which is thallium for these crystals. When a high energy photon of interest is incident with the crystal, the photon can excite an activator site within the crystal past its band gap energy. After a short time, the activator will de-excite and emit photons corresponding to its band gap energy, called scintillation photons. These photons are of lower energy and are in the visible spectrum. A photosensitive device, a silicon photomultiplier (SiPM) in the case of CITIES,

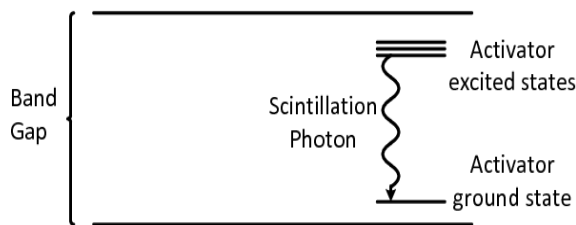


Figure 1: Simple depiction of activator excitation where energy is low in the ground state and high in the excited states.

is then used to collect these photons and generate a current pulse which is proportional to the initial energy of the high energy photon of interest. Figure 1 depicts the activator's band gap.

After the current pulse is generated by the photosensitive device, the signal is processed by a charge sensitive preamplifier (CSP) which produces a saw-tooth voltage pulse corresponding to the current pulse it was given. Now the initial high energy photon has been converted into a voltage which is still proportional to its initial energy. The signal

undergoes more processing to convert it into a useable signal. This signal is then converted into a digital signal and managed by the FPGA and flight computer subsystems. A block diagram for the single channel of the system used for the 2018 HASP flight is shown in figure 2.

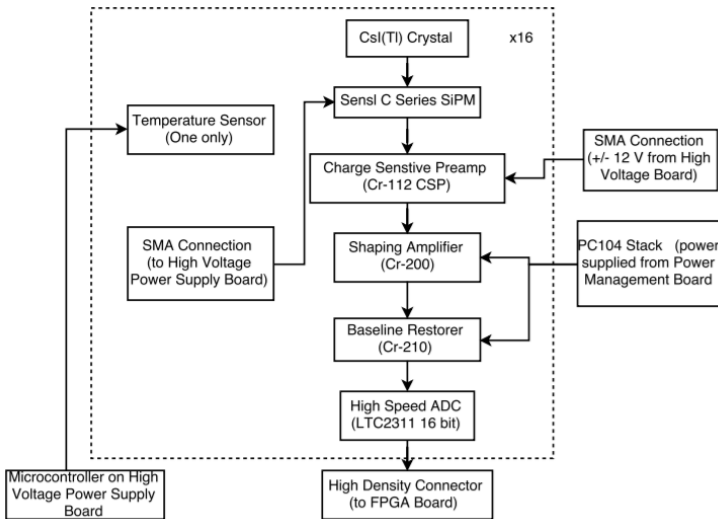


Figure 2: Block diagram of the detector system for the HASP 2018 flight. The actual engineering model was a single channel prototype of the overall 16 channel design.

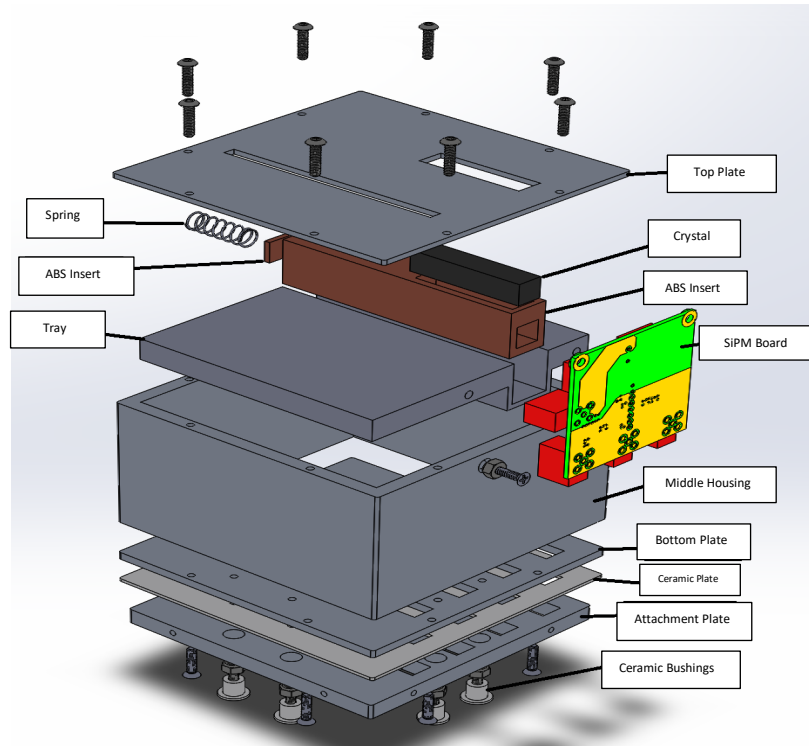


Figure 3: A 3D SolidWorks model of the 2018 iteration of CITIES.

## HAXDT Description

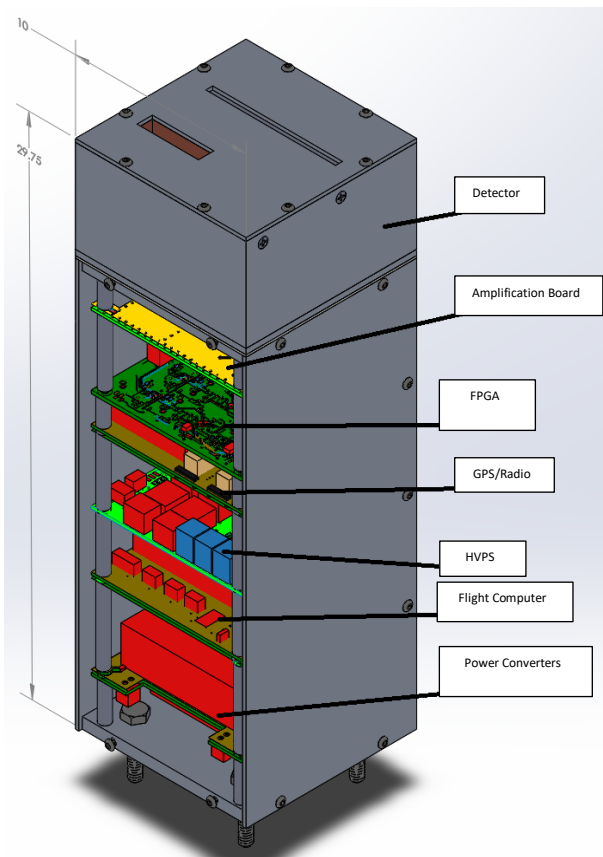


Figure 4: A 3D SolidWorks model of the 2017 iteration of HAXDT. Dimensions in centimeters.

The HAXDT payload was designed to closely resemble the integrated CubeSats that will be used for the EXACT and SOCRATES missions. In addition to CITIES, the rest of the payload, implemented as a PC/104 stack, had the following components:

- Novatel OEM615 GNSS receiver
- Artix A7 FPGA/Digilent Cmod A7 evaluation board
- FreeWave MM2-T Radio for communication
- Various additional boards for power regulation and data processing.

The ultimate goal of CITIES is to prove that an alternative navigation solution can be obtained by combining information received from sensors measuring fluxes of charged particles. Provided the time arrival of these particles can be precisely characterized in a way that can be represented as a distinctly binned rate (i.e., a signal that consists of detected event rates), the concept of relative positioning can be applied. This is all based on the assumption that cooperating spacecraft are equipped with similar detectors capable of picking up the same information that is being observed. With this information, one detector's observed rates can

be correlated with another's to obtain an estimate of the amount of time the detected radiation took to propagate from one detector to the other. Similarly, CITIES should also be able to measure the energies of individual hard X-ray photons from the sun as a method to investigate flare-accelerated energy distributions. It is not known how flares accelerate ions and electrons to such high energies, but it is known that accelerated electron populations produce high-energy ("hard") X-rays via the bremsstrahlung process. Hence, studying hard X-rays can serve as a diagnostic tool for energy release and can inform space weather models of coronal mass ejections by explaining and exploring their origins. Furthermore, CITIES should be capable of measuring the time of arrival of individual photons at microsecond timescales to investigate the acceleration time of solar flares.

In past iterations, HAXDT was designed to conform to the CubeSat generic structure standards. Using an internal PC/104 stack was also an effort to emulate the interface requirements of a real CubeSat. CITIES is situated on top, as seen in Figure 4, with the PC/104 stack extending below.

These boards all share common power rails and use the same computer bus. The PC/104 serves as a relay for power and general communications throughout the payload. The stack itself consists of commercially available components, including the flight computer, FPGA, GPS, and radio. The detector's front end is based on a thermalized nuclear particle detection board circuit designed by Cremat engineers. Originally designed for a four-channel instrument, this circuit was multiplied and spread onto a sixteen-channel (two-board) design located in the detector housing. Timestamps are based on the UTC time packets obtained from the GPS receiver. The initial time at power-up is obtained from these packets and the time is routinely updated thereafter.

The onboard FPGA is an Artix A7 chip on a Digilent Cmod A7 evaluation board which is integrated into a PCB with components for analog to digital conversion of incoming pulses and voltage regulation. This FPGA receives pulses from the amplification and CITIES detector via MMCX cable where high-speed 16-bit Analog to Digital Converters (ADCs) integrated into the circuit board convert the signal. The FPGA then characterizes these pulses by fitting them to a gaussian curve and recording parameters for the fit such as the amplitude, an estimated error, and a timestamp with 0.2 microsecond precision. These parameters are used to characterize the photon which initially produced the pulse. Upon initialization, the FPGA waits for a GPS lock to start its count and checks this lock to maintain a constant clock. Once the FPGA has processed a pulse, it writes it to an onboard microSD card for storage which is retrieved after the flight. This data will be sent back via radio to a ground station in the final iterations of this design.

The central processing unit is a BeagleBone Black rev. C microcomputer running on a Debian operating system. This unit was chosen mainly because of its versatility and legacy at the University of Minnesota as a flight computer for autonomous aerial vehicles. The BeagleBone communicates to a NovAtel OEM615 GPS connected via UART. The GPS gives data on the latitude, longitude, altitude, time up to a second precision, and the number of satellites the GPS was able to lock on to. The BeagleBone is able to control the detector system and radio as well as monitor the overall health of the payload via various temperature sensors within the payload. The BeagleBone also checks if there is communication with the Freewave MM2-T radio. If there is communication, the flight computer is able to send data from the payload upon request. This data includes temperature data, a current working software version, and GPS information. The BeagleBone is also able to reprogram remotely via the onboard radio as it can receive a software patch from a ground station and implement changes in the onboard code. This allows for the ability to remotely fix or modify any parts of the code on the BeagleBone throughout the flight. The BeagleBone is also able to turn on the secondary payload after the payload is above 70,000ft. The flight computer runs two pieces of code, the Goldy Legacy Architecture Derived Operating System (GLADOS) and Aura. Aura is the main flight computer code which handles all sensor interfacing and the state machine of the payload. GLADOS is the controller for Aura and handles reprogramming. GLADOS also ensures that Aura is operational after a reprogramming attempt is made. If the reprogramming fails and Aura is not operational, GLADOS will switch Aura to a previous working version so the whole system will still be operational.

A downlink method independent of telemetry is used to transmit the on-board GPS/temperature data to a ground station via a 915 MHz radio link. The FreeWave MM2-T radio receives data from the flight computer to be sent to the ground station. All data is also stored in the on-board memory to check packet quality upon retrieval of the payload. Ideally, the internal data should match

downlinked data. The ground station consists of an omni-directional antenna, a parabolic antenna, a tri-pod, and a computer. Via the LED readout on the MM2 radio, the ground station team is able to know when the link is established and broken.

## **Payload Performance**

Most of the performance expectations were met during ground testing at the Student Payload Integration at the Columbia Scientific Ballooning Facility. The FPGA recorded data onto the SD card and radio performance was verified during the thermal vacuum tests. Furthermore, the GPS maintained a lock during the tests and the detector itself was tested with a radiation source prior to the thermal vacuum test and was found to be functioning properly. Onboard health, GPS, and software version data was received via radio during most of the tests.

Issues were encountered during the tests despite other successes. A component on the FPGA board (specifically, an operational amplifier) was found to be improperly rated for the temperature range of the tests, so the data the FPGA was recording was inaccurate and did not match the results from tests performed prior to thermal vacuum testing. During the first test, the payload suffered a brownout from the HASP gondola in the middle of a reprogramming attempt of the flight computer. This caused Aura on the flight computer to become corrupted and the flight computer stopped working altogether. Serial and radio communications were lost during the first test because of this. The radio communication was regained after the test when the code for the flight computer was reuploaded. The serial communication was not reestablished before the second test due to a faulty RS-232/TTL converter chip. This faulty chip and the faulty op-amp were replaced during the period between payload integration and the beginning of flight operations.

Current draw within the payload also became an issue during the payload integration. Initially, the detector system would be turned off upon powerup and the flight computer would turn the detector on once it was done initializing. When the FPGA was turned on, however, a big increase in the current draw would cause the entire 5V rail in the payload to dip. This caused the flight computer to reset and initialize again, which would send it into an infinite loop of flight computer initialization. It was determined to leave the detector system turned on during flight computer initialization and for the entirety of the flight.

In the period between the payload integration and the flight operations, a component on the FPGA was found to have faulted, but the FPGA as a whole was still operable. The only issue with this was that the FPGA would heat up at an irregularly high rate. Because a thermal stress test of the payload is critical for both the SOCRATES and EXACT missions, it was determined that this would be an opportunity to test a “worst case scenario” of heating within the payload. An analysis of this heating is included later in the report.

Due to changes in the flight date, it was determined that the HAXDT team could not stay to operate the radio ground station during the flight. This posed no issue to the team as communications had been successfully tested on a previous HASP flight, and reprogramming of the flight computer via the radio could be done on the ground without the need to be in flight. Reprogramming was tested and validated during testing at the payload integration while the payload was not yet integrated

with the HASP gondola. While the HAXDT team was not in attendance for the flight, the payload was still able to be monitored via serial downlink of temperature, GPS and health data. The current draw and voltage was also monitored via the HASP telemetry readings. During the flight, the payload communication operated normally. Current draw and voltage increased as temperatures increased within the payload during float which was expected.

The CITIES detector performed well for most of the flight. The detector failed unexpectedly after the payload was powered on for 9.5 hours. This did not affect the rest of the payload. The unexpected failure of the detector was due to the failure of the SiPM bias line which was discovered upon post-flight payload testing. The bias line failure was determined to be the root cause of the detector failure after all other systems were determined to be functioning normally. This failure was due to the internal heating of the payload. A DC-DC switching converter chip which supplies the bias line was not rated for the highest internal temperatures the payload experienced. The detector performance is discussed in more detail later in the report.

The overall performance of the payload during the flight provided many insights into the effectiveness of the current designs. Data from the detector was collected for the majority of the flight which allowed for an in-depth analysis of detector performance through a broad temperature range which had not been done until this point. The FPGA allowed for fast processing of the incoming data from the detector which helps achieve a mission goal of fitting 200 incoming pulses per second for a single channel. This FPGA implementation will be refined and expanded to operate on up to 8 detector channels for the SOCRATES and EXACT missions and will be duplicated for a total of 16 channels per satellite. With the exception of the SiPM bias line, all systems endured the extreme heating within the payload and were functional post-flight.

### **Problems Encountered and Lessons Learned**

The 2018 HASP flight proved to be instrumental in the development of the CITIES detector system and its supporting hardware. The results of this flight have given direction to the subsequent redesign of the payload subsystems. The foremost lesson learned was the importance of environmental testing and the data collection that comes from it. The temperature data taken from the boards will help give a rough correlation for the detector performance to the temperature of the detector. It also allowed for the testing of the system in a non-convective environment. This highlighted the need for more rugged components within some of the electrical systems. With a non-convective atmosphere in low-earth orbit (LEO), any heating issues like the one encountered during this flight could result in reduced functionality or the termination of the satellite. With a more robust thermal mitigation design and more rugged components, the limits at which the payload can function will be greatly increased.

The need for system robustness and ruggedness is not limited to thermal mitigation, however. With the unexpected brownout that happened during payload integration, the need for a failsafe during reprogramming became extremely prevalent. Without the ability to have multiple flight computers onboard, a failsafe in the code had to be implemented. This also highlighted the need for hardware redundancy where a code failsafe is not an option or is not satisfactory. The biggest problems with this are physical space constraints on circuit boards and the ability to switch between pieces of hardware. With the size of the payload being limited to a 3U CubeSat form, there may not be room



to include redundant components for every critical piece of hardware. Major components such as the BeagleBone, FPGA, radio, and GPS receiver are rather large with respect to the whole structure and there is not enough space to for duplicates of these components within the payload. Therefore, these and any other components must be chosen and designed such that they are rugged and protected enough to survive the environmental conditions expected in LEO. This can be done by checking all available specifications for each component to make sure they can withstand the environmental conditions, choosing components with space heritage, and by providing thermal mitigation to components which tend to heat up such as processors or linear regulators. Furthermore, environmental testing will show which components need to be replaced or have thermal mitigation in place for them. The other concern with redundancy has to do with switching between redundant components. There are limited options for power and limited signals which can be used to switch on redundant components available. Therefore, various switches or electrical flip-flops will need to be implemented in order to properly switch between faulty and working components. The robustness and redundancy concerns are currently being addressed by the team.

## Results Summary

### Board Temp Through Flight

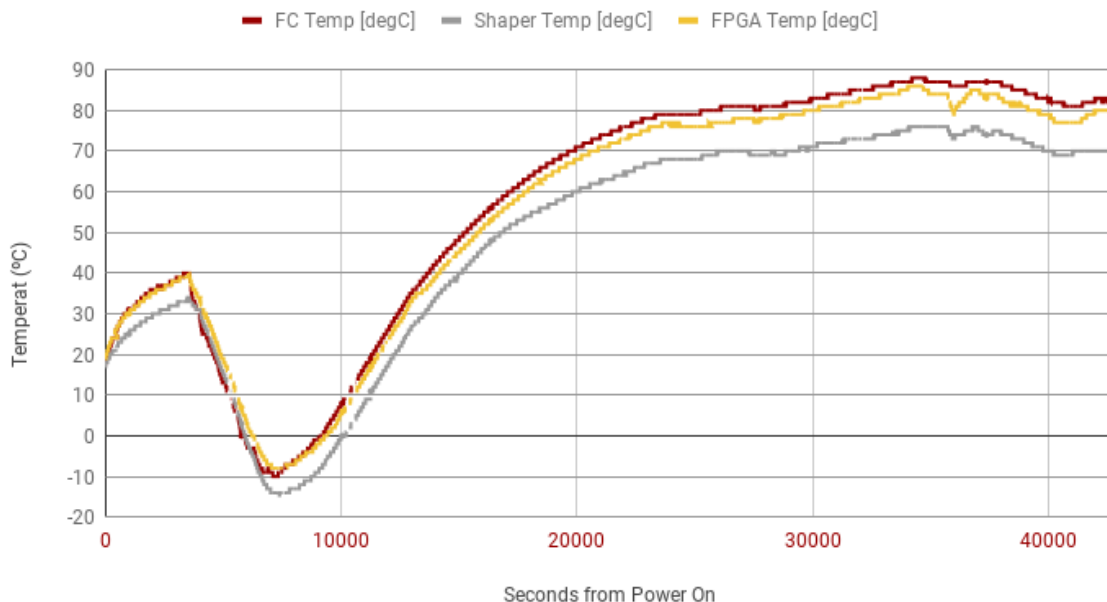


Figure 5: Board temperature over time during the flight.

As can be seen in Figure 5, the flight computer (FC) board reached the highest temperature at approximately 88°C at its peak during float. Though the FPGA was introducing more heat than what was normally expected, the FPGA board did not have the highest peak temperatures. This is most likely due to other components on the flight computer board such as the GPS and processors on the BeagleBone which add more heat to the flight computer board. The flight computer board was consistently the hottest board during the thermal vacuum tests, so with extra heat introduced,

the flight computer remained at a higher temperature than the FPGA board by  $\sim 3^{\circ}\text{C}$  on average. These graphs show that the flight computer board and FPGA board will be the most important boards to add thermal mitigation to. The amplification and shaping board was the coldest throughout the flight as it was away most of the components that heat up considerably.

As mentioned previously, the reprogramming of the flight computer could not be validated on the HASP flight. Instead, this was tested and validated during the team's independent testing. Initially, when the ground station requested the software version number, the flight computer would send only the version number.

```
what packet do you want to send?
(D)etector data, (B)urn Wire
(TP) Temp Packet, (GP) GPS Packe
(E)xit
V
32
what packet do you want to send?
(D)etector data, (B)urn Wire
(TP) Temp Packet, (GP) GPS Packe
(E)xit
```

*Figure 6: Ground station code requesting software version number*

Being as there were no patches which needed to be added to the flight computer code at this point, it was decided that it was necessary to inject a little school spirit into the flight computer code. Thus, the following changes were made.

```

//creates packet saying what software version is running
const char* getReproVersion(int Reprogramming_Mode)
{
    size_t len = 0;    //size of packet
    len = snprintf (NULL, len, "%d",Reprogramming_Mode);
    char *version = (char*)calloc (1, sizeof *version * len + 1);
    if (!version) {
        fprintf (stderr, "%s() error: virtual memory allocation failed.\n", __func__);
    }
    if (snprintf (version, len + 1, "%d",Reprogramming_Mode) > len + 1)
    {
        fprintf (stderr, "%s() error: snprintf returned truncated result.\n", __func__);
        return NULL;
    }
    return version;
}

//creates packet saying what software version is running
const char* getReproVersion(int Reprogramming_Mode)
{
    size_t len = 0;    //size of packet
    len = snprintf (NULL, len, "%d, !!!!!GO GOPHERS!!!!",Reprogramming_Mode);
    char *version = (char*)calloc (1, sizeof *version * len + 1);
    if (!version) {
        fprintf (stderr, "%s() error: virtual memory allocation failed.\n", __func__);
    }
    if (snprintf (version, len + 1, "%d, !!!!!GO GOPHERS!!!!",Reprogramming_Mode) > len + 1)
    {
        fprintf (stderr, "%s() error: snprintf returned truncated result.\n", __func__);
        return NULL;
    }
    return version;
}

```

Figure 7: Comparison between the flight computer code before (top) and after (bottom) reprogramming. These changes are implemented in a patch sent via radio for reprogramming.

Once a patch was made with these changes, the ground station sent the command to reprogram to the flight computer along with the desired patch. The flight computer then reprogrammed so that the next time the command requesting the software version was sent, the flight computer would send the new packet outlined in the code above with a new version number. This new packet was requested and was successfully sent.

```

what packet do you want to send?
(D)etector data, (B)urn Wire
(TP) Temp Packet, (GP) GPS Packet
(E)xit
V
33, !!!!!GO GOPHERS!!!!
what packet do you want to send?
(D)etector data, (B)urn Wire
(TP) Temp Packet, (GP) GPS Packet
(E)xit

```

Figure 8: Updated version number with additional school spirit included.

The CITIES detector system collected measurements for a total of 9 hours and 34 minutes. During this time, the FPGA processed 6.7 million voltage pulses. These voltage pulses are either direct measurements of incident high energy photons or electronic noise. As with any detector system, CITIES collects background noise. This background noise presents itself in the spectra produced by CITIES and can often obscure relevant photon measurements. On the HASP flight, the background noise appeared in two separate places; one noise peak occurred as was expected in the low energy part of the spectrum, and another noise peak introduced itself in the high energy part of the spectrum. These peaks are shown in the histogram below.

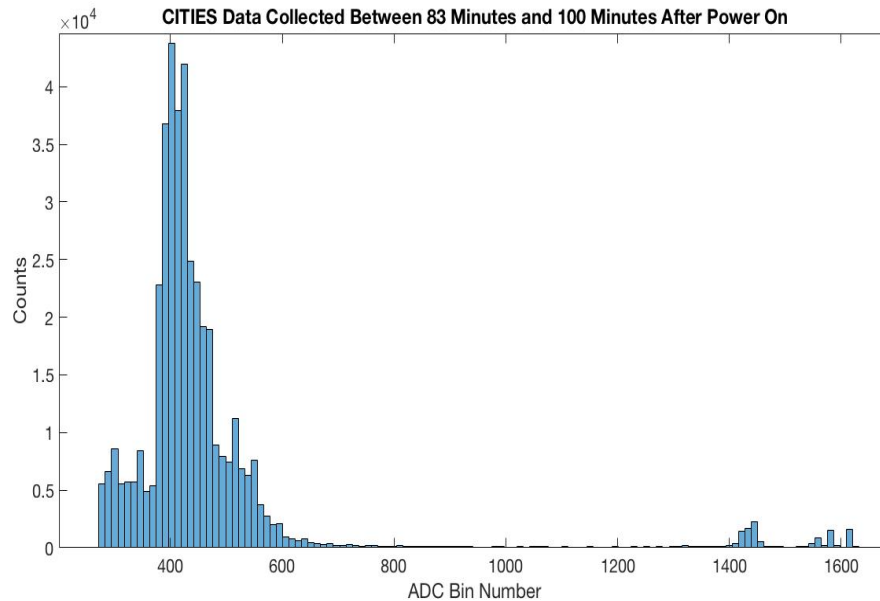


Figure 6: The histogram above depicts the energy spectrum generated from data collected between 83 and 100 minutes after the system was powered on. The data is binned according to an ADC bin number which is proportional to the amplitude of the voltage pulse generated by the CITIES system. The amplitude of a generated voltage pulse is roughly proportional to the energy of the incident photon. The first noise peak is clearly visible between bins 400 and 600. This peak will be referred to as the “noise floor” and is present in the low energy part of the spectrum. The second peak is visible between bins 1400 and 1450. This peak will be referred to as the “noise ceiling” and occupies the high energy area of the spectrum.

The noise floor peak is always observed in spectra measured by CITIES and is the direct result of electrical noise that is amplified by the charge sensitive preamplifier. The noise ceiling peak is a previously unobserved feature in the spectra measured by CITIES, but we suspect it can be attributed to an error in the FPGA curve fitting algorithm or, again, electronic noise. The noise ceiling peak does not appear when the voltage pulses from the shaper are processed by a standalone multi-channel analyzer (MCA). In order to understand more about the possible sources of this noise, the position of both peaks was tracked as a function of time. The position of the peaks was taken to be the bin value at which the maximum number of counts occurred. In figure 6, the noise floor peak reached a maximum value of  $4.374 \times 10^4$  counts in bin 405. In the same figure the noise

ceiling peak reached a maximum value of 2289 counts in bin 1440. The same measurements were made on the two peaks throughout the flight, and the position were then plotted versus time.

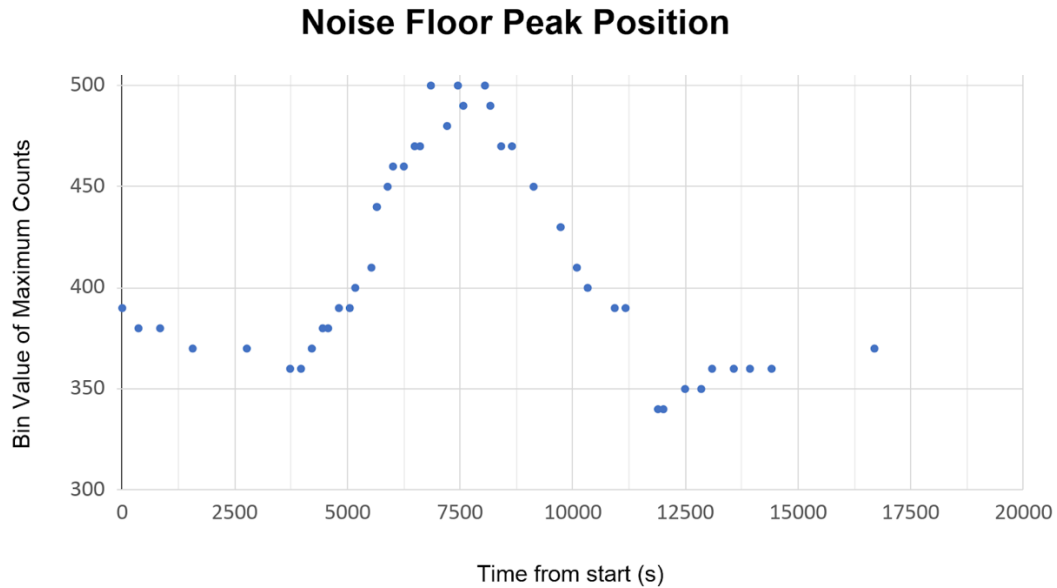


Figure 7: The graph above shows the position of the noise floor peak as a function of time. The position reaches its maximum value at  $7500 \pm 250$  seconds after power on, then returns to a bin value of  $360 \pm 50$  and remains there for the duration of operation of the detector.

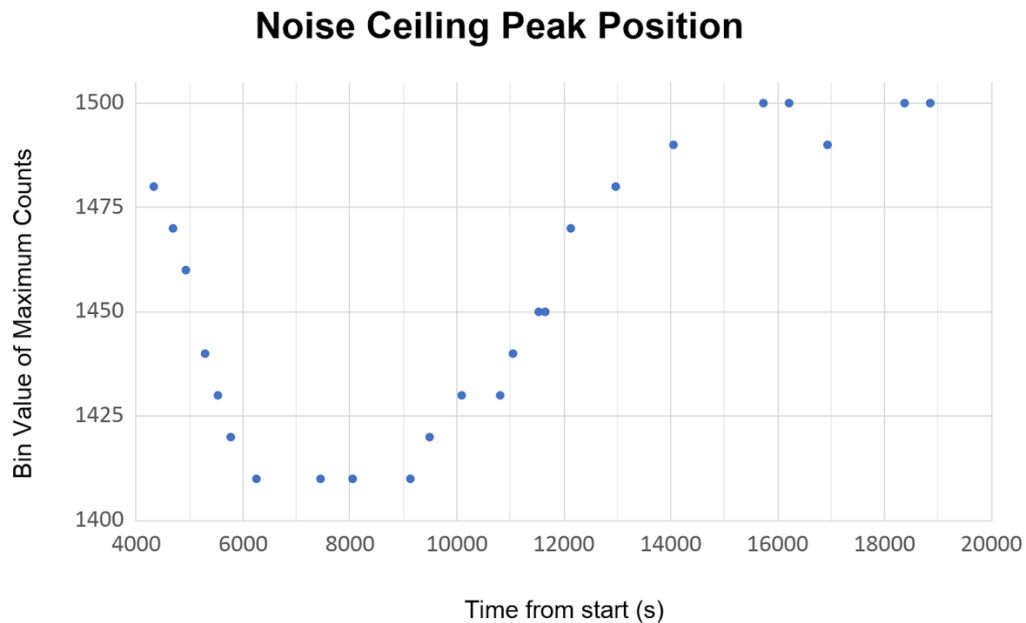


Figure 8: The graph above shows the position of the noise ceiling peak as a function of time. The position reaches its minimum value between 6000 and 9000 seconds after power on, with the center of that range occurring at  $7500 \pm 250$  seconds after start.

Tracking the noise peaks shows that each peak hits its relative extrema at nearly the same time, which occurs at 7500 seconds after the system was powered on. However, their behavior is opposite. The position of the noise floor increased and reached a maximum at the same time the noise ceiling decreased and then reached a minimum. This difference in behavior indicates that the noise floor and the noise ceiling likely originate from different sources, but the fact that they reach their relative extrema at the same time suggests that they are both influenced by similar external factors. In this case, it is believed that both sources of noise are influenced by temperature. The temperature of the amplification board was measured during flight at a frequency of 0.5 Hz. The shaper board is spatially the closest temperature gauge to the SiPMs.

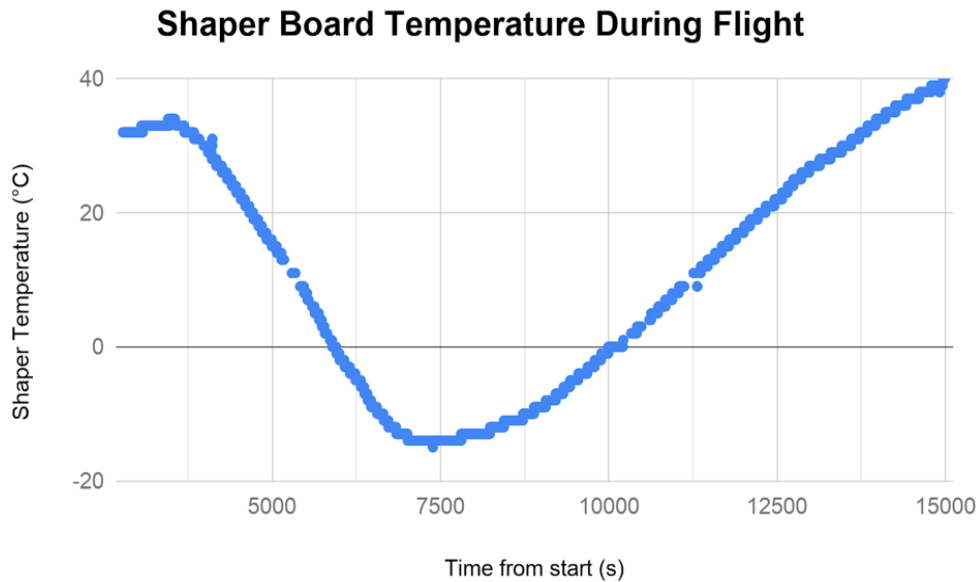


Figure 9: The graph above shows the temperature measured on the shaper board as a function of time since the system was powered on. The temperature reaches a minimum value of  $-15^{\circ}\text{C}$  at 7392 seconds after power on. The temperature was between  $-13^{\circ}\text{C}$  and  $-15^{\circ}\text{C}$  from 6844 to 8235 seconds from power on.

Based on the data presented above and the fact that most sources of electrical noise are temperature dependent, the peak in the noise ceiling was found to be noise introduced internally. If the noise ceiling peak was in fact not noise at all but rather the measurement of some incident high energy photons, it would be expected for that peak to display the opposite behavior with temperature. If the SiPM bias voltage is kept at a fixed value and the temperature of the SiPMs is decreased, the relationship between voltage pulse amplitude and incident energy is shifted up due to the shrinking of the band gap within the SiPM. This means that the reduction of SiPM temperature shifts peaks of the same energy to a higher ADC bin, which is the behavior we observed from the noise floor. However, the opposite behavior was observed with the noise ceiling peak. A decrease in temperature reduced the ADC bin at which the high energy peak appeared. Such a decrease in bin value indicates that the noise ceiling is in fact noise and not an external source.

An additional anomalous behavior was observed at the end of the detector data. The last data point was observed at 9 hours and 34 minutes after the system was powered on. However, the system was not powered down until 2 hours and 17 minutes after this. The spectrum produced at that time indicates that CITIES was no longer capable of measuring any high energy pulses, and that even noise in the high energy part of the spectrum was not present. This behavior is characteristic of an electrical failure within the detector system. As mentioned earlier, it was determined during post flight testing that the SiPM bias voltage supply line was cause of this failure.

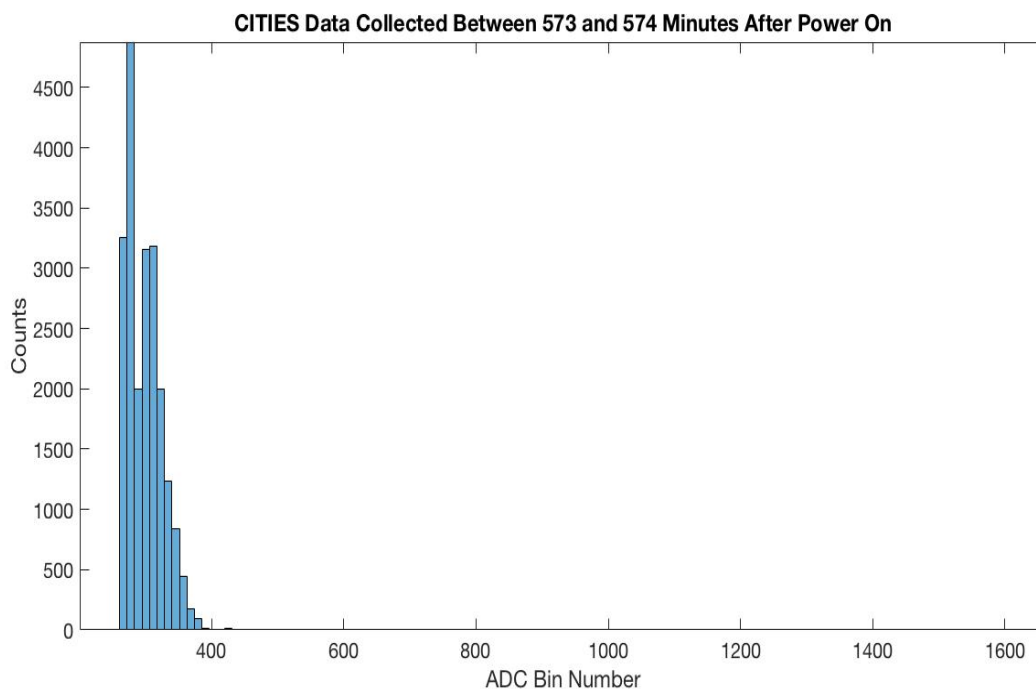


Figure 10: End of operation spectrum from the CITIES detector. The high energy part of the spectrum is entirely devoid of all counts, even the smallest background noise counts which would still be expected. Bin 425 is the highest bin for which any counts at all were collected.

The absence of further spectral features other than those already mentioned indicates that the measurements made with CITIES during flight are that of the background, which lacks any significant sources of high energy photons. This directly corresponds to data from the Geostationary Operational Environmental Satellite (GOES) observatory which detected very little solar activity during the flight. The background measurement produced is what was initially expected from this flight, and this leads to the conclusion that the measurements made with CITIES during the flight reasonably correspond with the expected measurements.

## Conclusions and Future Work

The results from the 2018 HASP flight provided insight into both the successes and failures of the CITIES detector system as these flights have for years. With the approaching launch of SOCRATES, these designs are nearing their final flight-ready designs. The HASP flight has validated the FPGA as a method of data processing and exposed flaws in both hardware and

software designs. The thermal mitigation and robustness of the system are currently being worked on and developed. The detector system is currently being expanded up to 8 channels for a full implementation of the CITIES detector. The designs for the whole system will be refined in further testing with the data collected on HASP as a foundation for the development.

## Student Involvement

Below is a table of all students associated with the 2018 HASP mission and their demographic information.

Name	Start Date	End Date	Role	Student Status	Race	Ethnicity	Gender	Disability
Abigail Valero	Summer 2017	Present	Chief Engineer	Undergraduate Senior	Caucasian	Hispanic	Female	Dyslexia
Kyle Houser	Feb 2018	Present	HASP Lead	Undergraduate Junior	Caucasian	Non-Hispanic	Male	None
Ricardo Saborio	Jan 2017	Present	Payload Systems Software Co-Lead	Undergraduate Junior	Caucasian	Hispanic	Male	None
Joel Runnels	Sept 2015	Present	Technical Consultant (Detector Engineering and physics) Payload Lead	Graduate Student	Caucasian	Non-Hispanic	Male	None
Samuel Drehmel	Spring 2017	Present	Detector Systems Physicist (Calibration and testing)	Undergraduate Senior	Caucasian	Non-Hispanic	Male	None
Jenna Burgett	Spring 2017	Present	Project Manager	Undergraduate Junior	Caucasian	Non-Hispanic	Female	None
Kaj Erickson	Spring 2018	Present	Detector Systems Lead (Calibration and testing)	Undergraduate Senior	Caucasian	Non-Hispanic	Male	None
Megan Birch	Summer 2017	Present	Detector Systems Physicist (Calibration and testing)	Undergraduate Senior	Caucasian	Non-Hispanic	Female	None



Jacob Beno	Fall 2017	Present	FPGA Lead	Undergraduate Junior	Caucasian	Non-Hispanic	Male	None
Runsheng Ma	Summer 2017	Present	FPGA Team Member	Undergraduate Sophomore	Asian	Non-Hispanic	Male	None
Inho Jong	Summer 2017	Present	FPGA Team Member	Undergraduate Senior	Asian	Non-Hispanic	Male	None
Yuya Teshima	Summer 2018	Present	FPGA Team Member	Undergraduate Sophomore	Asian	Non-Hispanic	Male	None
Yahya Alhinai	Spring 2018	Present	FPGA Team Member	Undergraduate Junior	Caucasian	Non-Hispanic	Male	None
Andrew Mosin	Spring 2017	Present	Payload Systems Software Co-Lead	Undergraduate Junior	Caucasian	Non-Hispanic	Male	None
Athanasios Pantazides	Spring 2017	Present	Payload Systems Hardware Lead	Undergraduate Senior	Caucasian	Non-Hispanic	Male	None
Lukas Zumwalt	Summer 2017	Present	Communications Lead	Undergraduate Junior	Caucasian	Non-Hispanic	Male	None
Garrett Ailts	Summer 2018	Present	MURI Team Lead	Undergraduate Junior	Caucasian	Non-Hispanic	Male	None
Ryan VanDaalwyk	Summer 2017	Present	Structures Team Member	Undergraduate Senior	Caucasian	Non-Hispanic	Male	None
James Cannon	Summer 2018	Present	Structures Team Lead	Undergraduate Junior	Caucasian	Non-Hispanic	Male	None
Alex McKeever	Spring 2018	Present	Payload Systems Software	Undergraduate Sophomore	Caucasian	Non-Hispanic	Male	None
Alexis Valencia	Spring 2018	Present	Detector Systems Physicist	Undergraduate Senior	American Indian/Alaskan Native	Hispanic	Female	None
Marie Wulff	Summer 2018	Present	Payload Systems Hardware	Undergraduate Sophomore	Asian	Non-Hispanic	Female	None

Below is the table of all past students associated with the 2015, 2016 and 2017 HASP missions and their current information.

<b>Name</b>	<b>Degree Obtained</b>	<b>Graduation Date</b>	<b>Current Activity</b>
Gaurav Manda	Bachelor of Electrical Engineering	Spring 2018	Graduate School: University of Michigan-Ann Arbor
Aaron Nightingale	Bachelor of Electrical Engineering	Spring 2018	Graduate School: University of Minnesota
Maxwell Yurs	B.S. Physics	Spring 2018	Graduate School: University of Minnesota
Jeffrey Chaffin	B.S. Physics	Spring 2017	Current employer: UC: Santa Cruz Title: Doctorate Student
Ilya Zubarev	B.S. Physics	Spring 2017	Unknown
Luke Granlund	B.S. Physics	Spring 2017	Current employer: National Geospatial Intelligence Agency Title: Unknown
Gjerda Rhodes-Humphries	B.S. Technical Writing and Communications	Spring 2017	Current employer: Graco Title: Technical Writer
Seth Frick	Master of Aerospace Engineering	May 2015	Current employer: Honeywell Aerospace Title: Radar Systems Engineer
Josiah Delange	Bachelor of Aerospace Engineering	December 2015	Current employer: Digi International Title: Cellular Firmware Engineer
Charles Denis	Bachelor of Aerospace Engineering	May 2016	Current employer: Quality Bicycle Products Title: Design Engineer
Justin Seifert	Bachelor of Aerospace Engineering	May 2016	Current employer: Carl Zeiss Industrial Metrology Title: Applications Engineer
Jacob Gustafson	Bachelor of Aerospace Engineering	May 2016	Current employer: UTC Aerospace Title: Software Engineer
Nick Janak	B.S Physics Bachelor of Aerospace Engineering	December 2015 May 2016	Current employer: Carl Zeiss Industrial Metrology Title: Applications Engineer M.S Mechanical Engineering (In Progress)

Nicholas Sloan	Bachelor of Aerospace Engineering	May 2016	Current employer: Generation Orbit Title: Structures Engineer
Ethan Arendt	Bachelor of Aerospace Engineering	May 2016	Unknown
Brian Hanson	Bachelor of Aerospace Engineering	May 2016	Unknown
Benjamin Setterholm	Bachelor of Aerospace Engineering	May 2016	Graduate School: University of Michigan, Ph.D. in Astrophysics

### Papers and Presentations

Conference/ Location of Publication	Title of Article or Poster	Authors and/or Presenters	Date Published or Presented
SPIE 2017 in San Diego, California	Developing a Detector Model for the Experiment for X-ray Characterization and Timing (EXACT) CubeSat	Trevor Knuth	August 2017
Small Satellite Conference 2018 in Logan, Utah	Cesium Iodide Thallium-doped Incident Energy Spectrometer (CITIES): A Hard X-Ray Detector for CubeSats	Jenna Burgett Maxwell Yurs	August 2018

### Acknowledgements

The University of Minnesota HASP/HAXDT team gratefully acknowledges the technical advice and support from the staff of ASTER Labs, Inc. We also thank the Louisiana Space Consortium and NASA's Balloon Program Office for the continued support of the HASP flight. We would like to thank Kale Hedstrom and Dr. James Flaten for their technical advice and encouragement. Finally, we acknowledge the NASA/Minnesota Space Grant Consortium for providing funding to the HASP payload development and the University of Minnesota. The generous resources we've received for this project encourage us to continue working and innovating.

While the authors gratefully acknowledge the aforementioned individuals, the views and conclusions expressed in this report are those of the authors alone and should not be interpreted as necessarily representing the official policies, either expressed or implied, of any organization.

## References

- [1] P. T. Doyle, The Development of a Simulator System and Hardware Test Bed for Deep Space X-ray Navigation, vol. Master of Science Thesis, Minneapolis, MN: Department of Aerospace Engineering and Mechanics, University of Minnesota, Twin Cities Campus, 2012.
- [2] P. T. Doyle, D. Gebre-Egziabher and S. I. Sheikh, "The Use of Small X-ray Detectors For Deep Space Relative Navigation," in SPIE Nanophotonics and Macrophotonics for Space Environments, San Diego, 2012.
- [3] C. S. Hisamoto and S. I. Sheikh, "Spacecraft Navigation Using Celestial Gamma-Ray Sources," *Journal of Guidance, Control, and Dynamics*, vol. 38, pp. 1765-1774, 2015.
- [4] NASA, "NASA Technology Roadmaps - TA5 (2015)," NASA, Washington, D.C., 2015.

## Appendix A: HAXDT Secondary Payload Report

### Introduction

The 2018 flight of HAXT contained a secondary payload which was an AlphaSense Optical Particle Counter (OPC) from the University of Minnesota's High Altitude Ballooning Team. The AlphaSense OPC is being used by the UMN High Altitude Ballooning team to characterize high altitude particle concentrations as part of a Multidisciplinary University Research Initiative (MURI) project sponsored by the Air Force. The MURI team will use this data to create more accurate simulations of how atmospheric particulates and fluctuations in the free-stream flow conditions interact with hypersonic boundary layers. These simulations will better predict laminar-turbulent transition and thus aide in hypersonic vehicle design.

### Secondary Payload Description

The secondary payload consisted of the AlphaSense OPC-N2 and an external battery which was controlled with a relay by the HAXDT main payload's flight computer. The secondary payload was turned on at an altitude of 24km and remained turned on for the duration of the flight.

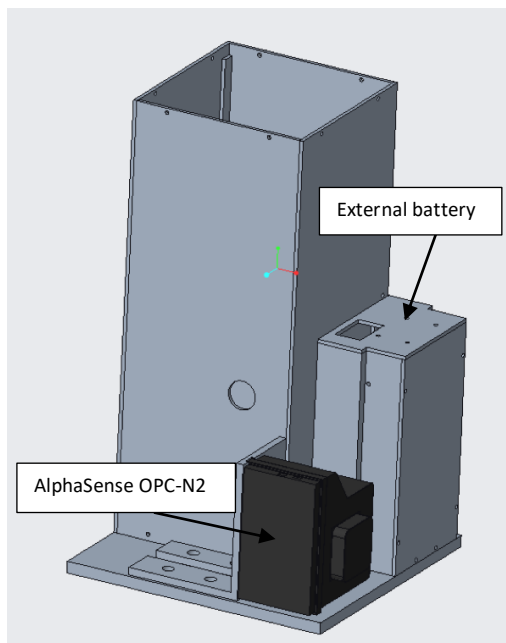


*Figure A1: A 3D SolidWorks model of the secondary payload with the main HAXDT structure*

The MURI team's goal on this year's HASP balloon flight was to collect data on the particulate content of the upper atmosphere. In particular, they wanted to measure particle concentrations and size distributions in the atmosphere at altitudes of 24-37 km. These measurements were to be done in-situ, on-board the gondola, using a low-cost OPC. Leading up to the HASP launch, the MURI team had been perfecting its own ballooning techniques to consistently reach such altitudes in the atmosphere, as well as investigating the OPC in regard to calibration and integration with existing ballooning payloads. The opportunity of flying the OPC on HASP 2018 was then extremely appealing to the MURI team as it would ideally result in a large data set of particle measurements at relevant altitudes, in addition to making measurements in an environment that the MURI team had yet to accomplish, which was floating at an altitude for an extended period of time.

The nature of the measurements made by the OPC are based on light-scattering techniques, where individual particles are detected and sized accordingly, resulting in samples consisting explicitly of particle number counts per second (# particles/sec) per size; quantities such as particle concentration can then be obtained from post-analysis using the sample count and sample flow rate.

## Results

Ultimately, the flight was a success. Particle measurements were made from ~24 km to ~37 km, then for a duration of ~5+ hours at ~37 km, resulting in over 60,000 samples. Furthermore, the OPC that was flown on HASP was the first sensor that had been calibrated before flight, meaning that the collected data gave the most well-understood results to-date.

The OPC categorizes particles into 16 separate size bins, ranging from 0.38-17  $\mu\text{m}$ ; the initial analysis of the flight data suggested that all size bins, except the smallest (0.38-0.54  $\mu\text{m}$ ), appeared to be zero meaning that, from an altitude of 24-37 km, the OPC only detected particles in the size range of 0.38-0.54  $\mu\text{m}$ . The concentration as a function of altitude for this size bin is shown in Figure A2.

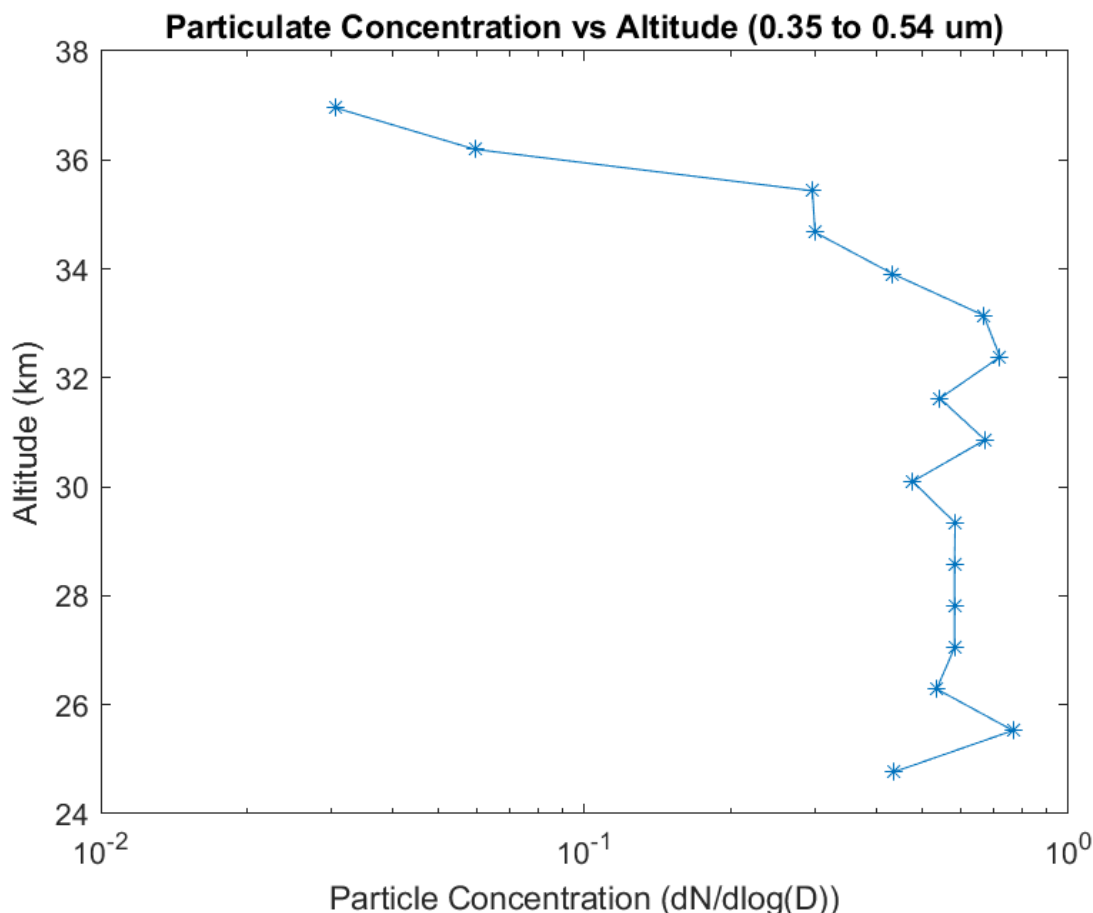


Figure A2: Plot of particle concentration as a function of altitude. This plot shows that from an altitude of approximately 24-37 km, the particle concentration appears to have a constant order-of-magnitude, somewhere between  $10^{-1}$  and  $10^0$  particles/cm<sup>3</sup>. Over an altitude of 34 km, the concentration appears to decrease by approximately two orders-of-magnitude, to less than  $10^{-1}$  particles/cm<sup>3</sup>.

The magnitudes shown in this plot are fairly consistent with Renard et. al. 2015, which consist of measurements made at similar altitudes from a weather balloon [1]. In contrast, the size distribution presented by Renard et. al. shows the presence of larger particles, up to 0.9  $\mu\text{m}$ , in concentrations of similar magnitude to the smaller particles described above. They also show the

existence of much larger particles, 3-7.5  $\mu\text{m}$ , in concentrations of the order less than  $10^{-2}$  particles/cm<sup>3</sup>. However, note that these measurements were made over France, high above a sand plume, using a much more sophisticated OPC.

Figure A3 shows the concentration as a function of the time elapsed between the beginning of sampling to the end of sampling. The OPC is in ascent from  $t=0$  to approximately  $t=150$  mins. Between  $t=150$  mins and  $t=450$  mins, the OPC is at its apogee of  $\sim 37$  km, where the smallest magnitude of concentration was measured and appeared to remain fairly constant. Past  $t=450$  mins, the OPC is in descent, then gets powered off at approximately  $t=550$  mins. Of note is the symmetry shown in Figure A3, between approximately  $t=100$ , near the end of ascent, and  $t=525$  mins, shortly after descent begins, which suggests that the OPC is indeed detecting changes in its environment in a consistent manner.

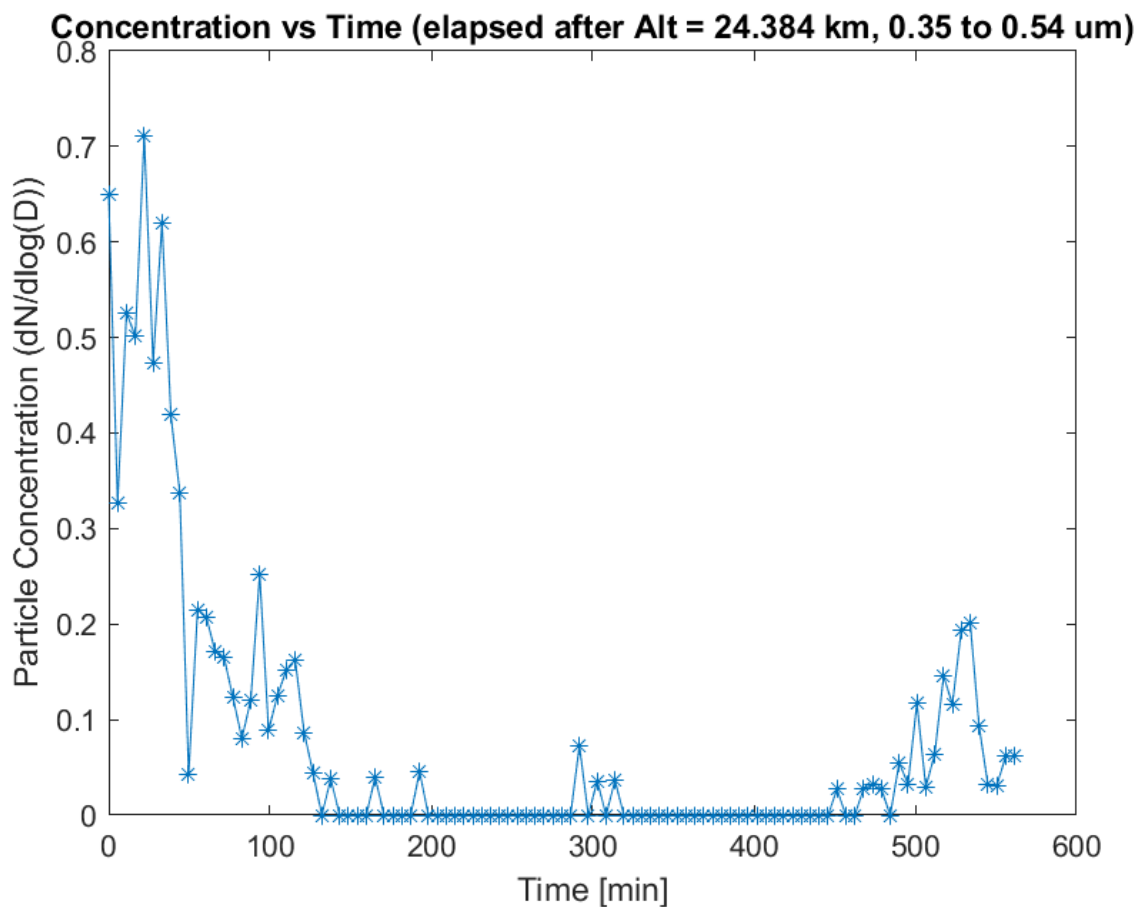


Figure A3: Plot of concentration of particles versus time. The symmetry of concentrations can be seen before  $t=100$  and after  $t=525$ .

## Conclusion

This data suggests that sub-micron particles dominate the size distribution in the upper atmosphere where the HASP gondola was flown and as a result suggests that calibration of these instruments should be focused on sub-micron particles sizes, keeping in mind that calibration of optical particle counters are extremely crucial (and expensive). However, it should be noted that a potential source

of error has not been accounted for in these measurements, namely the effect of a rarefied environment (low pressure and density) on the operability of the OPC. The calibration mentioned earlier was done only at 1 atm conditions; as the environment becomes more rarefied, the OPC may not be able to account for the significant changes in density and pressure, resulting in miscalculated flow rates (and thus concentration) and inertial disposition of the particles (and thus undetected particles). Inertial disposition could be the reason that the OPC did not detect any particles larger than 0.38-0.54  $\mu\text{m}$ , as shown in Renard et al. This is because larger particles have greater inertia, so at low pressure and density, they may tend to not follow the streamlines within the flow path of the OPC, and ultimately, not arrive at the “detecting zone” of the sensor. Characterizing such phenomena that occur in a rarefied environment is of great importance to the MURI project, and efforts are currently being made to simulate this environment for calibration.

With this year being the first that MURI has participated in HASP, the value of the opportunity became evermore evident. The team plans to submit a proposal for a fully MURI-dedicated payload for next year’s HASP flight, in addition to developing a particulate measuring payload that is designed to be optimized for integration with HASP specifically.

#### **References:**

[1] J.-B. Renard, F. Dulac, G. Berthet, T. Lurton, D. Vignelles, F. Jégou, T. Tonnelier, C. Thauray, M. Jeannot, B. Couté, R. Akiki, N. Verdier, M. Mallet, F. Gensdarmes, P. Charpentier, S. Mesmin, V. Duverger, J. C. Dupont, T. Elias, et al. 2015. LOAC: a small aerosol optical counter/sizer for ground-based and balloon measurements of the size distribution of atmospheric particles - Part 2: First results from balloon and unmanned aerial vehicle flights. *Atmospheric Measurement Techniques*. 8:1261–1299.